RSC Advances

PAPER

View Article Online
View Journal | View Issue

Cite this: *RSC Adv.*, 2025, **15**, 25497

Dual surface functionalised curcumin-shellac nano-delivery system with enhanced antimicrobial action†

Saba S. M. Al-Obaidy, [ab] Gillian M. Greenway, [a] Saule Kalmagambetova [c] and Vesselin N. Paunov *[c]

We report a strong boost of the antimicrobial action of curcumin (CUR) upon encapsulation in sterically stabilized shellac-based nanoparticles (NPs) with cationic surface functionalisation. The CUR-loaded shellac NPs were fabricated by solvent attrition and co-precipitation by mixing an aqueous solution of ammonium shellac and an ethanolic solution of curcumin followed by a pH drop from 8 to 5 in the presence of the sterically stabilising polymer Poloxamer 407 (P407). The surface functionalisation of the produced curcumin nanocarrier was done by subsequent doping with the water-insoluble cationic surfactant octadecylthrimethylammonium bromide (ODTAB). Optimal nanocarrier stability was obtained at a fixed ratio of (0.25 : 0.2) wt% of shellac : poloxamer 407 concentrations. Shellac NP formulations containing 0.01–0.07 wt% concentration range of encapsulated CUR with 0.25 wt% shellac at pH 5 were successfully produced and examined for the efficiency of CUR encapsulation and its release from these nanocarriers. We studied the antibacterial action of CUR-NPs before and after the cationic surface functionalisation to evaluate the encapsulation efficiency, the role of the nanocarrier components and surface properties on its antibacterial, antiyeast and antialgal action. The antimicrobial effect of the surface functionalised CUR loaded-shellac NPs was evaluated on different proxy microorganisms, including *E. coli*, *C. reinhardtii* and *S. cerevisiae*. The cationic coating of the shellac NPs strongly enhanced the antimicrobial effect of the encapsulated CUR for all the examined microorganisms. We envisage that the enhanced effect is due to the strong electrostatic attraction of the coated CUR-loaded shellac NPs and the anionic surface of the cell walls which promote the nanocarrier accumulation directly on the microbial cell membrane and the local delivery of CUR which increased its bioavailability. This nanotechnology-aided amplification of the antimicrobial effect of CUR may potentially offer new antialgal, anti-yeast and antibacterial formulations based on natural ingredients as shellac and curcumin without the use of conventional antibiotics.

Received 7th May 2025
Accepted 20th June 2025

DOI: 10.1039/d5ra03212a

rsc.li/rsc-advances

[a]*Department of Chemistry, University of Hull, HU6 7RX, UK*

[b]*Department of Chemistry, College of Science, University of Babylon, Hilla 51001, Iraq*

[c]*Department of Chemistry, School of Sciences and Humanities, Nazarbayev University, Kabanbay Batyr Ave 53, Astana, 010000, Kazakhstan. E-mail: vesselin.paunov@nu.edu.kz*

† Electronic supplementary information (ESI) available: (i) Fig. S1: The chemical structure of curcumin (CUR) in: (A) in acidic and natural medium, (B) in alkaline medium; (ii) Fig. S2: Average particle size (A) and zeta potential (B) of 0.25 wt% shellac NPs coated with 0.05 wt% ODTAB; (iii) Fig. S3: The Fourier transform-IR spectrum of free curcumin, 0.03 wt% CUR-NPs, and shellac NPs with P407 at a range of wavenumber 600–4000 cm^{-1}; (iv) Fig. S4: The absorption spectrum of curcumin, free shellac, curcumin loaded shellac NPs and poloxamer 407 using UV-vis spectrophotometry technique at range (700–200) nm; (v) Fig. S5: The calibration curve of varies concentrations of CUR at 426 nm in DI water using UV-vis spectrophotometer; (vi) Fig. S6: (A) The effect of coating shellac NPs with different concentrations of ODTAB on the size and zeta potential at pH 5. (B) Scanning electron microscopy picture of shellac NPs coated with 0.05 wt% ODTAB. The NPs was coated with carbon; (vii) Fig. S7: (A) The effect of coating 0.03 wt% of CUR-loaded shellac NPs with different concentrations of ODTAB on the size and zeta potential at pH 5. (B) Scanning electron microscopy picture of 0.01 wt% of CUR-loaded shellac NPs after coating with 0.05 wt% of ODTAB; (viii) Fig. S8: The viability of *C. reinhardtii* cells upon incubation for 15 min, and 2 hours at pH 5.5 with different amounts of shellac NPs coated with ODTAB at room temperature; (ix) Fig. S9: The viability of yeast cells incubated with non-loaded ODTAB-coated shellac NPs of different concentrations at different incubation times: 15 min, 2 h, 4 h, and 6 h at pH 5.5; (xi) Fig. S10. The cytotoxic effect of non-loaded ODTAB-coated shellac NPs of different concentrations on *E. coli* for several different incubation times at room temperature. The shellac NPs were not loaded with CUR. The ratio of shellac:ODTAB in the NPs is fixed to 5 : 1. The *x*-axis shows the variation of the shellac and ODTAB concentrations for these experiments; (xii) Fig. S11: SEM images of microbial cells after being incubated with 0.025 wt% ODTAB coated 0.125 wt% shellac NPs for 4 h at pH 5.5. (A and B) algal cells, (C and D) yeast cells, and (E and F) *E.coli* cells; (xii) Table S1: Statistical analysis data for the effect of ODTAB-coated CUR NPs on microalgae based on the results in Fig. 4E; (xiii) Table S2: Statistical analysis data for the effect of ODTAB-coated CUR NPs on yeast based on the results in Fig. 5E; (xiv) Table S3: Statistical analysis data for the effect of ODTAB-coated CUR NPs on E.coli based on the results in Fig. 6E. See DOI: **https://doi.org/10.1039/d5ra03212a**

Introduction

Curcumin (CUR) is a natural product found in *Curcuma longa* L. turmeric plant and is widely used in the natural medicinal practice[1,2] with broad spectrum antimicrobial activity including antiviral, antibacterial, antimalarial and antifungal activities.[3] It also exhibits anti-inflammatory, antioxidant, anticarcinogenic activity,[4–13] inhibits lipid peroxidation and to prevent the haemoglobin oxidation.[14] It shows activity against myocardial infarction and atherosclerosis,[15] and skin conditions like psoriasis, skin carcinogenesis, dermatitis and scleroderma, rheumatoid arthritis,[15] multiple sclerosis,[15] Alzheimer's disease,[16] inflammatory bowel disease,[17] cystic fibrosis[18] and others.[15,19–21] Curcumin exist in keto or enol form (Fig. S1, ESI†) and has a poor solubility in water.

Nanocarriers for efficient drug delivery of pharmaceuticals have been widely developed due to their ability to control the rate of drug release.[22,23] In order to enhance the curcumin bioavailability it has been encapsulated within biodegradable polymeric microspheres, liposomes, polymeric and lipo-NPs, hydrogels and cyclodextrin.[24–31] Curcumin has been formulated in nano-delivery systems with three biocompatible polymers, chitosan, pluronic surfactant, and alginate using ionotropic pre-gelation followed by polycationic cross-linking.[32] Curcumin has also been loaded in lipophilic bilayer of dihexyl phosphate (DHP), cholesterol and egg yolk phosphatidyl choline (EYPC). Cationic lipid/polymer conjugate *N*-dodecyl chitosan-*N*-[(2-hydroxy-3-trimethylamine) propyl] (HPTMA) chloride has been used to coat liposomes with a size of 73 nm. These nanoparticles had the ability to penetrate the cancer cells and release the sustained content in about 10 hours.[33] Curcumin has also been encapsulated within various, mostly biodegradable polymers.[34] Due to its biodegradability and biocompatibility, Poly(D, L-lactic-*co*-glycolic)(PLGA) is commonly used for drug delivery purposes.[35–38] Curcumin was loaded on PLGA nanospheres using the emulsion-evaporation technique to yield particles of size 264 nm and 77% encapsulation efficiency was found with 15% loading curcumin capacity and enhanced curcumin oral bioavailability by 9 fold.[39] Song *et al.* used solid dispersion technique to load curcumin into methoxy poly(ethylene glycol)-*b*-poly(ε-caprolactone-*co*-*p*-dioxanone) as amphiphilic micelles.[40]

The CUR-loaded micelles had a small size of 30 nm with an entrapment efficiency of more than 95%, where the drug loading was 12%. These micelles showed slow release of about 80% of curcumin content during 300 hours.[40] Another way was used to increase the curcumin solubility by conjugating it to small amino acid molecules, as well as to both synthetic and natural hydrophilic polymers. Tang *et al.* succeeded in conjugating curcumin to two short oligo(ethylene glycol) chains through β-thioester bonds that are labile with the existence of esterase (Curc-OEG) and intracellular glutathione. The Curc-OEG conjugates particles contained 25 wt% curcumin, the curcumin micelles had a size of 37 nm with release amount of conjugated curcumin less than 12% using hydrolysis during 24 hours at pH 5.0 and 7.4 which demonstrating good stability of this nano-micelles in PBS.[41] Table 1 displays some of the *in vitro* characteristics of curcumin loaded with different nanocarriers.[32,39,42–46] As it can be seen, curcumin was loaded with negatively charged nanocarrier which may repel with the negatively charged bacterial cell membrane. Common for these curcumin formulations is that negatively charged nanocarriers have poor adhesion to the cell membrane of bacteria and are not suitable for enhancing its antimicrobial action.

Shellac is a naturally derived resin which contains a complex mixture of hydroxy aliphatic acids and terpenoid acids, almost in an equal percentage.[47] As shellac resins are nontoxic, biologically degradable and hypoallergenic, they have a grown in importance.[48–51] Preparation of aqueous based shellac colloids have been reported by Krause and Muller[52] by using a high-pressure jet homogenisation technique. Shellac colloids with particle size of several hundred nanometres were formulated by Patel *et al.*[53] and Kraisit *et al.*[54] by using an antisolvent technique by using xanthan gum and chitosan, respectively to encapsulate silibinin and bovine serum albumin. Al-Obaidy *et al.*[55–57] fabricated sterically stabilised shellac NPs with cationic antimicrobial and antibiotic payloads. They showed enhanced antibacterial effect when benchmarked to solutions of berberine, chlorhexidine or vancomycin at identical concentrations. This approach was taken further by Weldrick *et al.*[58–60] by encapsulating the antifungal agent Amphotericin B in Alcalase-coated shellac nanocarriers which proved very efficient in clearing biofilms of *Candida albicans*. The same approach was found to be effective on removal of bacterial biofilms.[59–61] Using surface-functionalised antimicrobial nanocarriers have recently been used to repurpose old antibiotics and other antimicrobials which can potentially overcome antimicrobial resistance.[60,62–67]

Table 1 Summary of recently reported nanocarriers for curcumin within their parameters (particle size, zeta potential, encapsulation efficiency)

Nanocarrier for CUR encapsulation	Particle diameter/nm	ζ-Potential/mV	E. E./%	CUR content/%	References
PLGA/poloxamer	160 ± 31	−19 ± 1	90 ± 2	—	42
Poly (D, L-lactic-*co*-glycolic)	264	−4.3 ± 0.3	77	15	39
MPEG-P(CL-*co*-TMC) copolymer	28 ± 1	0.11 ± 0.34	96 ± 3	14 ± 1	43
Alginate (ALG), chitosan (CS), and pluronic F127	100 ± 20	—	14.34	—	32
Shellac	100–250	−30	40–80	—	46
SLNs consists of stearic acid, poloxamer, dioctyl sodium sulfosuccinate, ethanol and lyophilized with mannitol	450	—	70	—	44

In this study, we developed CUR-nanodelivery system with high bactericidal efficiency against *E. coli*, as well as antifungal and antialgal cells activity using a shellac-based dual-functionalised nano formulation.[55–57] Fig. 1 shows the encapsulation steps of the CUR into the shellac nanocarriers during their preparation and subsequent surface functionalisation. The entrapment of the CUR in the nanocarriers is due to hydrophobic and H-bond interactions within the shellac matrix components. Here, we designed a novel preparation protocol for aqueous based shellac NPs loaded with CUR, and stabilised by using surface active copolymer, poloxamer 407 (P407) to ensure that they are sterically stabilised. P407 is a non-ionic co-polymer made up of poly(ethylene oxide) (PEO)–poly(propylene oxide)–(PPO) poly(ethylene oxide) (PEO), which is used in many pharmaceutical formulations as a dispersing and emulsifying agent[68,69] due to its low toxicity.[50,70]

Further we performed an additional surface doping with an ultra-low concentration of a water-insoluble cationic surfactant, octadecyl trimethyl ammonium bromide (ODTAB), delivered from ethanolic solution to charge-reverse the shellac NPs to net positive charge. Note that the ODTAB is directly deposited on the shellac NPs surface in a secondary step while the already formed sterically stabilizing polymer layer in the first step remains functional as the nanocarrier maintained its steric stability while being surface charge-reversed by the ODTAB doping. This steric stabilisation of the nanocarriers also complements the cationic surface functionalisation by the ODTAB coating which ensures that it accumulates electrostatically to the negatively charged cell walls of microbial cells and delivers locally a high CUR concentration that enhances its antimicrobial action. The slow release of CUR from the shellac NPs cores allows its potential use in wound dressings. We followed the release kinetics of the CUR and characterised its antimicrobial action before and after surface functionalising of the CUR-loaded shellac NPs with ODTAB. Our experiments demonstrated that this nanocarrier design can strongly enhance the action of CUR compared to an aqueous dispersion of equivalent concentration of the non-loaded CUR-loaded shellac NPs as well as ODTAB-coated non-loaded shellac NPs.

CUR exhibits antimicrobial activity through multiple mechanisms specific for the different genres of microorganisms: (i) CUR antimicrobial activity is strongly linked to ROS overproduction, which damages microbial cells by oxidizing essential biomolecules. CUR disrupts the microbial redox homeostasis by increasing intracellular ROS levels, leading to oxidative damage to lipids, proteins, and DNA. This oxidative stress overwhelms the microbial antioxidant systems resulting in cell death. In bacteria curcumin not only generates ROS, damaging membranes and biomolecules, but it also chelates iron, promoting Fenton reactions that further enhance ROS production.[71,72] Curcumin's hydrophobic nature allows its intercalation into microbial membranes, causing increased membrane permeability, leakage of cellular contents and enhanced susceptibility to ROS.[73] CUR also disrupts fungal cell membranes and mitochondria, increasing ROS and leading to apoptosis-like death.[74] This ROS

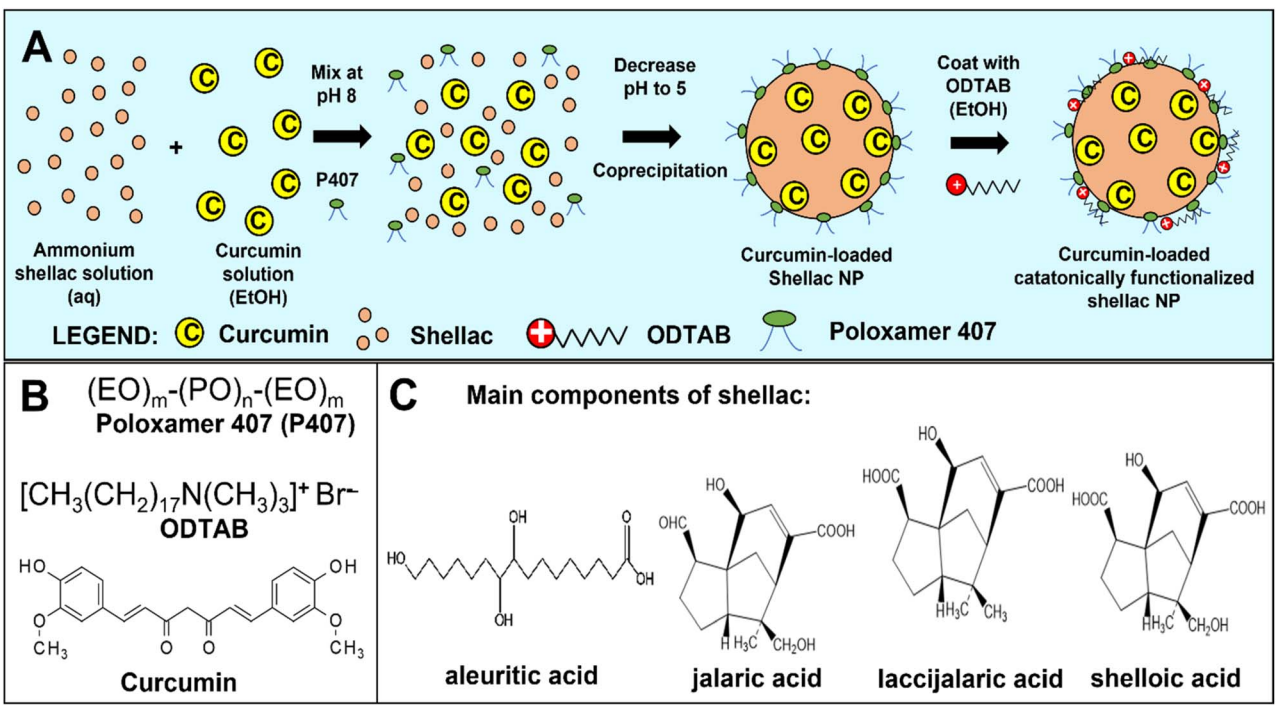

Fig. 1 (A) Schematics of a dual step preparation of cationically functionalised curcumin-loaded shellac nanoparticles (CUR-ShNPs). The CUR-ShNPs were stabilised sterically with a surface-active polymer, poloxamer 407 added in the first preparation step. The cationic surface functionality of the particles was done by subsequent lacing with the NPs system with a small amount of ethanol solution of a water-insoluble cationic surfactant, octadecyltrimethyl ammonium bromide (ODTAB). (B) Structural formulas of the constituting materials for the preparation on of curcumin-shellac nanocarriers: P407, ODTAB, CUR and (C) the main components of shellac.

generating mechanism, combined with membrane disruption makes CUR and its nanoformulations a potent broad-spectrum natural antimicrobial agent. Here we explore the antimicrobial action of the CUR-loaded shellac nanoparticle formulations on *E. coli*, microalgae *C. reinhardtii*, and yeast cells, *S. cerevisiae*, respectively, as three proxy microorganisms for bacteria, fungal cells and microalgae.

Materials and methods

Materials

Deionised water (DI) purified by reverse osmosis and ion exchange from a Milli-Q water system (Millipore, UK) was used in all our studies. Its surface tension was 71.9 mN m^{-1} at 25 °C, with measured resistivity less than 18 MΩ cm^{-1}. Shellac was used in a soluble form as the ammonium salt (SSB Aqua Gold™, solid content 25%) at pH > 7. The ammonium shellac solution was a gift from (Stroever Schellackbremen, Germany). Curcumin ((CUR), 1,7-bis[4-hydroxy-3-methoxyphenyl]-1,6-heptadiene-3,5-dione) was purchased from Sigma Aldrich, UK. Poloxamer 407 (purified, 99%) and 3′,6′-diacetyl fluorescein (FDA), were supplied from Sigma-Aldrich, UK. Octadecyltrimethyl ammonium bromide (ODTAB) was supplied by Fluka Chemika, UK. The BacTiter-Glo microbial cell viability assay was purchased from Promega, UK.

Dulbecco's modified Eagle's medium (DMEM) and fetal bovine serum (FBS) and 0.25% trypsin-ethylenediaminetetraacetic acid (EDTA) were sourced from ThermoFisher Scientific (KZ). Corning 96-well TC treated flat bottom plates, Hoechst 33342 and Propidium Iodide were purchased from ThermoFisher Scientific (KZ). CellTiter 96® Aqueous One Solution Cell Proliferation Assay (MTS) and BacTiter-Glo™ bacterial cell viability kits were purchased from Promega, (Madison, USA). Human keratinocytes (HaCaT cell line) were ordered from AddexBio, code T0020001.

Preparation of algal, yeast and bacterial cultures

Chlamydomonas reinhardtii (cc-124 strain) was kindly provided by Flickinger group from North Carolina University, USA. The microalgae were cultured in Tris-Acetate-Phosphate (TAP) culture medium at 30 °C. The *C. reinhardtii* culture media consisted of TAP salts (NH_4Cl; $MgSO_4 \cdot 7H_2O$ and $CaCl_2 \cdot 2H_2O$), phosphate buffer solution (PBS) and Hutner's trace elements solution (EDTA disodium salt, $ZnSO_4 \cdot 7H_2O$, H_3BO_3, $MnCl_2 \cdot 4H_2O$, $CoCl_2 \cdot 6H_2O$, $CuSO_4 \cdot 5H_2O$, $FeSO_4 \cdot 7H_2O$, $(NH_4)_6Mo_7O_{24} \cdot 4H_2O$), all supplied by Sigma-Aldrich, UK. The microalgae suspension culture was incubated in the TAP media at pH adjusted to 7 while being illuminated for 72 h with a white luminescent lamp with a light intensity of 60 W m^{-2} under stirring with a magnetic stirrer at 60 rpm.[55–57,75,76] *C. Reinhardtii* suspension culture with a typical concentration 4×10^5 cells mL^{-1} was produced which was measured by cell counter (Nexcelom Cellometer Auto X4).[55–57,75,76] *Saccharomyces cerevisiae* was supplied by Sigma-Aldrich, UK. Then 1 mL of this hydrated yeast suspension (1 mg lyophilised yeast per mL of DI water) was added to 100 mL of autoclaved YPD culture media[47] consisting of peptone (Sigma Aldrich, UK), D-glucose, (Fisher Scientific, UK), and yeast extract (Oxoid ltd, UK), and incubated at 30 °C for 24–48 hours. *Escherichia coli*, sourced from Thermofisher (Invitrogen MAX Efficiency™ DH10B™) was used to produce a stock suspension by culturing with approximately 5×10^7 cells mL^{-1} in autoclaved Luria-Bertani medium[55–57] prepared by dissolving 0.5 g yeast extract, 0.5 g sodium chloride (Sigma Aldrich), and 1 g tryptone (Oxoid Ltd) in 100 mL DI water.

Preparation and ODTAB-surface functionalization of CUR-ShNPs

Shellac nanoparticles (ShNPs) were prepared from solutions of 0.25 wt% ammonium shellac solution at pH 8 with typically 0.2 wt% of P407 and subsequent adjustment of the solution pH from 8 to 5 using 0.1 M HCl drop-wise and stirring. 0.5 wt% curcumin (CUR) stock solution dissolved in absolute ethanol was loaded in the shellac solution with P407 at pH 8 which was then followed by lowering of the pH to 5 using the diluted HCl aqueous solution. Different overall concentrations of CUR (0.01, 0.03, 0.05, 0.07) wt% were added to a fixed mixture of shellac : poloxamer 407 with ratio of 0.25 : 0.2 wt% respectively at room temperature before the pH-induced precipitation. Typically, a formulation of 0.03 wt% of curcumin-loaded within ShNPs of ratio of 0.25 : 0.2 wt% shellac and poloxamer 407 was chosen to be used as a stock in other experiments. The surface charge of the ShNPs was reversed from negative (P407-coated CUR-loaded ShNPs) to positive by an adding a very low amount of the cationic surfactant ODTAB, which is insoluble in water. The ODTAB was delivered to the shellac NP suspension by drop-wise addition from 3% ODTAB in absolute ethanol. The water-insoluble ODTAB is deposited on the surface of the CUR NPs by hydrophobic and electrostatic interactions following the attrition of the solvent (ethanol) in the aqueous solution. Typically, we added small aliquots of 3% ODTAB in ethanol to the CUR NPs suspension until 0.05 wt% of ODTAB overall concentration was reached. The stability of the ODTAB coating was studied further as described in the next section.

Shellac NPs ζ-potential, size distribution and morphology characterisation

The average ζ-potential and the hydrodynamic diameter of shellac NPs with and without CUR were measured without further dilution by dynamic light scattering (DLS) and electrophoretic light scattering (ELS) using a Zetasizer Nano ZL (Malvern Instrument Ltd, UK). All quoted measurements were conducted in triplicates. The nanoparticles were also examined by transmission electron microscopy (TEM) (Joel 2010, Japan). For this purpose, the sample of the particle suspension after 10-fold dilution with DI water was drop-casted on carbon-coated copper grids after being negatively stained with 1% aqueous uranyl acetate and air dried. The sample was observed with a Jeol 2010 TEM at 200 kV using Gatan Ultrascan 4000 digital camera.

UV-vis spectroscopy and fourier transform infrared (FTIR) and study

To determine the curcumin loading percentage in the CUR NPs, a UV-vis spectrophotometry technique was used. A sample of the

CUR NPs was dissolved in alkaline solution (pH 8) and the UV-vis spectrum was scanned in the range 220–700 nm using a spectrophotometer Bio Lambda 10 (USA). FTIR spectroscopy was used to characterise CUR NPs and shellac NPs by using Thermo Scientific Nicolet 380 FT-IR, Hemel Hempstead (UK). This was also applied to confirm the adsorption of poloxamer 407 on shellac NPs surface and the interlocking of the CUR and the shellac matrix.

CUR encapsulation efficiency and loading in CUR NPs

The CUR encapsulation efficiency and loading was calculated by from the absorbance of the non-encapsulated curcumin solution obtained by filtering of the CUR NPs suspension through a 20 nm syringe filter using the UV-vis spectrophotometer and the use of a calibration graph of the absorbance (at 426 nm) of a series of standard CUR solutions of varying concentrations. The drug loading content and encapsulation efficiency were estimated as follows:

$$\text{Encapsulation efficiency } (\%) = \frac{[\text{total CUR} - \text{unencapsulated CUR}]}{[\text{total CUR}]} \times 100,$$

$$\text{CUR loading content}(\%) = \frac{[\text{total CUR} - \text{unencapsulated CUR}] \times 100}{[(\text{total CUR} - \text{unencapsulated CUR}) + \text{shellac} + \text{poloxamer}]}.$$

In vitro CUR release kinetics from CUR NPs

The release profile of the CUR from the suspension of CUR NPs was determined using a dialysis method. Typically, 50 mL of the CUR NPs suspension stock were dialyzed in a dialysis bag of 12–14 K MWCO immersed in a 200 mL DI water in an Erlenmeyer flask. The flask with the bag was stirred on an orbital shaker at 37 °C temperature and 100 rpm.

At fixed time points, 2 mL of the dialysed solution in the flask was taken and its UV-vis absorbance was measured at 426 nm. Absorbance measurements were done at 15, 30, 60, 120, 180, 240, 300, 360 and 1440 min. The cumulative percentage of released CUR was calculated using the equation

$$\%\ \text{CUR release} = \frac{M_{\text{released}}}{M_{\text{total}}} \times 100.$$

Here the amount of CUR released from the shellac NPs at time t is denoted with M_{released} and M_{total} is the total amount of CUR loaded.

SEM and TEM image acquisition of CUR-NPs treated cell samples

SEM images were acquired for cells and encapsulated shellac NPs coated with ODTAB. The cells were washed with DI water 3 times to remove the culture media by centrifugation at 3000–5000 rpm for 3 min; then they were deposited on dry Aclar sheets or poly-lysine coated glass coverslips followed by fixation with 2.5 w/v% glutaraldehyde for 2 h, by washing with cacodylate buffer, post fixed for 1 h in 1 wt% osmium tetroxide, washed again with a cacodylate buffer, and then rinsed with solutions of water and ethanol in steps starting from 50 vol% and up to absolute ethanol, and finally dried using critical point dryer. Before imaging they were coated with 10 nm carbon layer and imaged using scanning electron microscope ZEISS EVO 60 EP-SEM (Germany).

Antimicrobial activity of the non-coated CUR-loaded shellac NPs

To study the effectiveness of loading the drugs within shellac nanoparticles against *C. reinhardtii*, *S. cerevisiae*, and *E. coli* cells, a range of concentrations of CUR-loaded shellac nanoparticles and ODTAB coated CUR-loaded shellac nanoparticles were incubated in the presence of these cells for various incubation times at pH 5.5. Empty shellac nanoparticles without CUR payload (as a negative control) were incubated with the cells for different time intervals. The cell viability of *C. reinhardtii* and *S. cerevisiae* was measured after incubating 1.0 mL of cells with 15 μL of (5 mg mL^{-1}) of FDA solution in acetone for 10 min and washed 3 times with DI water by centrifugation at 3000 rpm. The fluorescence readout was done using a Nexcelom Cellometer Auto X4 cell counter. The luminescence of *E. coli* cells was measured after incubating the cells with series of concentrations of the nanoparticles loaded with CUR at different times. Typically, 100 μL aliquot of the standardised *E. coli* stock suspension was mixed with 100 μL of BacTiter-Glo™ bacterial cell viability reagent in white opaque 96-well microplate, and after a wash with DI water and being shaken for 5 min, the luminescence was measured using FLUOstar Omega instrument (BMG LABTECH, Germany).[77]

Cytotoxicity of non-coated and ODTAB-coated CUR NPs against human keratinocytes

Proliferation of human keratinocytes (HaCaT cell line) in the presence of various concentrations of ODTAB-coated CUR NPs were measured using the CellTiter 96® AQueous One Solution Cell Proliferation Assay (MTS). Equal aliquots of control and treated HaCaT cell suspensions were incubated into clear TC-treated 96-well plates at a density of 7500 cells per well in 100 μL of complete DMEM (90% DMEM and 10% FBS). The plates were incubated for 24 hours at 37 °C in a humidified atmosphere containing 5% CO_2 to allow for cell attachment and recovery. Cur NPs working solutions by diluting the 0.08% ODTAB-coated 0.05 wt% curcumin-loaded shellac NPs stock in complete DMEM to reach the final concentrations. After 24 h of incubation the media to the respective wells was carefully aspirated and replaced with 100 μL of each Cur NPs stock dilution in complete DMEM. Following the 24 hours treatment period, the medium in each well was changed and 10 μL of MTS reagent was added and incubated at 37 °C for 1.5 h, protected from light. Absorbance at 490 nm was measured using a FLUOstar Omega Microplate Reader after 1.5 h of incubation. Cell proliferation was calculated as a percentage relative to untreated controls. Cell viability was estimated using dual

staining with 1 μg mL^{-1} Hoechst 33342 solution and 1 μg mL^{-1} Propidium Iodide (PI) solution in PBS.

Hoechst and PI working solutions were prepared by diluting 10 μL of 1 μg mL^{-1} Hoechst and PI stock into 990 μL of PBS. After CUR NPs treatment for 24 h, the old medium was aspired and replaced with 100 μL fresh medium. An aliquot of 10 μL of Hoechst and 13 μL of PI working solution were added directly into each well and the plate was incubated for 30 minutes at 37 °C in the dark. The stained cells were images using a fluorescence microscope with DAPI and TRITC filter sets. Image analysis was done by ImageJ free software to determine the number of total (Hoechst) and dead (PI-positive) cells. The cell viability percentage was calculated using the following equation:

$$\%\ \text{viable cells} = \left(1 - \frac{\text{number of dead cells}}{\text{number of total cells}}\right) \times 100\%$$

Statistical analysis

Statistical analysis was performed using one-way ANOVA followed by Tukey's post-hoc test to assess pairwise comparisons across four independent groups. A two-way repeated measures ANOVA also with Tukey's multiple comparisons test was conducted to examine the effects of group ($n = 4$) and time ($n = 3$ time points) on the outcome variable. All analyses were conducted using GraphPad Prism software. The adjusted p-values were presented as significant (*) when $p < 0.05$, very significant (**) when $p < 0.01$, (***) highly significant when $p < 0.001$ and (****) highly significant when $p < 0.0001$. Statistical significance was stated directly in the corresponding figures using standard asterisk notation.

Results and discussion

Preparation and characterisation of CUR-loaded shellac NPs

Curcumin is almost insoluble in water and has a very poor bioavailability, rapid metabolism, low intrinsic activity, high rate of metabolism, and/or rapid elimination and clearance from the body.[78,79] In order to improve its solubility and bioavailability, curcumin was formulated into biodegradable shellac nanoparticles. Curcumin as a hydrophobic polyphenolic compound was encapsulated within shellac NPs by mixing shellac with curcumin and poloxamer 407 at pH 8 then reducing the pH to 5 by adding dropwise 0.1 M HCl. The shellac and curcumin coprecipitate due to hydrophobic–hydrophobic interaction as shellac is a hydrophobic material.[80] Curcumin is stable at acidic pH but unstable at neutral and basic pH.[81] Curcumin nanoparticles were formulated at size of 88 ± 29 nm with zeta-potential of −5 ± 1 mV. The CUR NPs are sterically stabilized by the poloxamer 407 adsorption layer which makes them less insensitive to pH changes and show good long-term stability despite the low magnitude of the zeta-potential. Fig. 2A and B show the particle hydrodynamic diameter distribution and the zeta-potential distribution of shellac NPs formulated by mixing the composition of 0.25 wt% of shellac

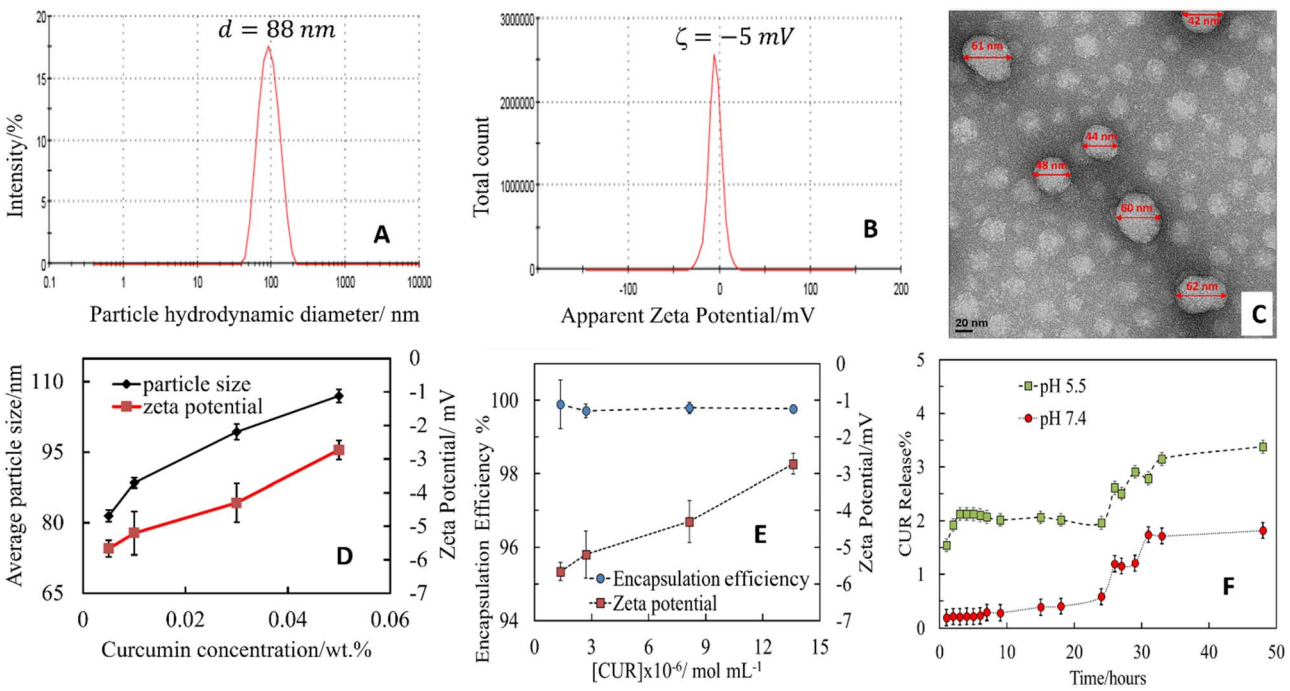

Fig. 2 (A) Particle hydrodynamic diameter and (B) zeta-potential distributions of shellac nanoparticles produced from an aqueous solution of 0.25 wt% of ammonium shellac and 0.2 wt% P407 by a pH drop from pH 8 to pH 5 before coating with ODTAB. (C) TEM of ODTAB-coated CUR-loaded shellac NP (CUR NPs)s; (D) the shellac NPs average hydrodynamic diameter and zeta-potential as a function of the CUR concentration. (E) The encapsulation efficiency percentage and average zeta-potential of different concentrations of CUR, loaded in shellac NPs at pH 5 at fixed shellac and P407 overall concentrations. The particles are not coated with ODTAB. (F) The release profiles of CUR from CUR NPs at two different values of the solution pH supported by an acetate buffer (5.5) and PBS (7.4).

with 0.2 wt% P407 at pH 8 and dropping the pH to 5. The PDI values of the CUR NPs samples are typically in the range 0.07–0.11. CUR-NPs sample was further examined by transmittance electron microscopy (TEM) as shown in Fig. 2C and confirmed that the particles exhibit a spherical morphology.

The TEM image of the shellac NPs suspension sample after drying shows an average particle size of smaller than the DLS measured hydrodynamic diameter. This is linked to the poloxamer coating in aqueous environment. Fig. 2D shows that standard shellac NPs composition can be loaded up to 0.05 wt% CUR and at higher concentration an aggregation occurs. However, the zeta-potential decreased while the loaded amount of curcumin increased. The zeta-potential of these CUR-loaded shellac NPs is negative at pH 5 due to the partial dissociation of the –COOH groups of the shellac constituents. Note that ODTAB was not used here to coat the shellac NPs. The CUR NPs are sterically stabilised by the poloxamer 407 adsorption layer which makes them less insensitive to pH changes and show good long-term stability despite the low magnitude of the zeta-potential. CUR was encapsulated with the shellac NPs by following the protocol described above. Fig. 2E shows that the encapsulation efficiency of CUR at pH 5 was extremely high, over 99% and practically did not depend on the CUR concentration. In all experiments here CUR was encapsulated at pH 5 by using the same composition shellac and P407 (0.25 wt% : 0.2 wt%).

UV-vis and FTIR studies

The optical properties for shellac, curcumin, and curcumin -loaded NPs show distinct difference among samples. Curcumin solution (in water) looks turbid indicating substantial aggregation, while CUR-NPs suspension appears transparent yellow indicating the stabilisation of CUR-NPs and lower light scattering. UV-vis spectroscopy study proved the encapsulation of curcumin within shellac NPs. Curcumin has strong absorption at 426 nm (grey line, Fig. S4, ESI†). While shellac has very strong absorption in the UV region with no significant peaks (green line, Fig. S4, ESI†). CUR NPs shows the presence of two peaks, one broad peak in the visible region at around 440 nm, and the second appeared in UV region at 240 nm which belong to curcumin NPs (blue line, Fig. S3, ESI†). The appearance of the peak at 440 nm indicated that curcumin has loaded within shellac nanoparticles.

The FTIR spectrum of curcumin Fig. S4, ESI† (red line) shows one sharp peak at 3510 cm^{-1} demonstrating the presence of O–H. (C=C) and (C=O) vibration have strong peaks and were predominantly mixed at 1625 cm^{-1}. Asymmetric stretching vibrations of the aromatic ring (C=C ring) shows a strong band at 1601 cm^{-1}. The 1504 cm^{-1} peak is distributed to the (C=O), whereas enol C–O peak appeared at 1271 cm^{-1}. The other characteristic peaks are as follows: C–O–C peak at 1024 cm^{-1}, benzoate *trans*-CH vibration at 961 cm^{-1} and vibration *cis*-CH of aromatic ring at 712 cm^{-1}. All these results are in line with the literature reports.[82,83] CUR-NPs spectrum (blue line, Fig. S4†) shows a broad peak around 3350 cm^{-1} which belongs to the absorption of O–H stretching vibration band for shellac and curcumin molecules. Most curcumin principle peaks were fused with shellac NPs bands and shifted slightly. Few of curcumin peaks appeared, like C=O, enol C–O, and benzoate trans –CH peaks are assigned at 1514 cm^{-1}, 1279 cm^{-1}, and 962 cm^{-1} respectively. The presence of these peaks proposed that curcumin was encapsulated within the nanoparticles by hydrophobic interactions and had not chemically reacted with the shellac molecules.

Table 2 Curcumin loading percentage at pH 5 encapsulated with composition 1 (0.25 wt% shellac : 0.2wt% P407)

Mol mL^{-1} CUR loaded in shellac NPs formulation	Drug loading (%)
1.36×10^{-6}	5
2.70×10^{-6}	9.2
8.14×10^{-6}	23
1.36×10^{-5}	33.8

Curcumin encapsulation efficiency and drug loading content measurements

The encapsulation efficiency of curcumin within shellac NPs was calculated indirectly by determining the amount of curcumin in the supernatant after filtering samples using syringe filter of 20 nm pore size by using a calibration graph presented in Fig. S5 (ESI†) obtained by using UV-vis spectrophotometer. Fig. 2E shows that curcumin can be encapsulated within shellac NPs up to 100% at pH 5 with loading amount of 33.8% at 13.6×10^{-6} mol mL^{-1}, as can be seen in Table 2. The high trapping amount of curcumin within shellac particles is attributed to the high affinity between curcumin and shellac and the stabilizing effect of the poloxamer 407 molecules as they all contain hydrophobic parts.

In vitro curcumin release studies

In vitro curcumin release studies were conducted to determine the amount of released curcumin at a specific pH. Due to the insolubility of curcumin in water, a buffered surfactant solution was placed outside the dialysis bag with the CUR NPs. 0.45 wt% Cetyltrimethylammonium bromide (CTAB) was added to a buffer solution to maintain the solubility of curcumin after releasing throughout the dialysis bag.[84] Fig. 2F shows that curcumin releasing was very slow at pH 5.5 and was slower at 7.4, only about 3.5% was released after 2 days at pH 5.5 and a half of this amount at pH 7.4. The slow release could be attributed to the high affinity between the curcumin and the shellac nanoparticles material as they express hydrophobic–hydrophobic interaction, this confirms that shellac can be loaded with curcumin for sustained drug release with long-term drug activity as it could be used for many days as well as reducing the side effect of high drug usage.

Surface functionalization of shellac NPs

Modification of CUR NPs surface charge was achieved by coating nanoparticle surface with water-insoluble cationic surfactant (ODTAB). This altered the nanoparticle zeta potential

from negative to positive, thus increasing the accumulation of the coated CUR NPs on the microbial cell walls and consequently delivering a high local dose of curcumin. Fig. S2A and B (ESI†) shows that CUR NPs particle size undergoes a minor change from 95 nm to 105 nm by adding 0.03 wt% of ODTAB or higher. However, the zeta potential reverses from negative (Fig. 2B) to positive as shown in Fig. S2B (ESI†). We selected an overall 0.05 wt% of ODTAB to coat CUR-NPs in further experiments. We compared the size distributions of the shellac NPs coated with ODTAB and the CUR-NPs after ODTAB coating in Fig. S6A and B (ESI†) which indicated that CUR-NPs remain in the nanosized range over a wide range of ODTAB:shellac concentration ratios. The coated nanoparticles were imaged by a SEM, and a representative SEM image is given in Fig. S6B and S7B (ESI†) shows a spherical morphology of the CUR NPs.

Antialgal, antiyeast and antibacterial activity of CUR-loaded shellac NPs

Here, the studied ODTAB-coated CUR nanoformulations increase the accumulation of CUR at higher concentrations on the cell walls microbial cells (Fig. 4D, 5D and 6D) which enhances its antimicrobial potential action. We tested the antialgal, anti-yeast and antibacterial activity of the ODTAB-coated shellac NPs without CUR-loading for different ratios of the shellac and ODTAB. One can see from the Fig. S8–S10 (ESI†) that at the selected concentrations of ODTAB used, the empty nanocarrier (ODTAB-coated shellac NPs) has very low toxicity in the absence of CUR. This is despite their accumulation on the surface of the treated algae, yeast and *E. coli.* (Fig. S11, ESI†). The antialgal activity of CUR loaded shellac NPs was tested on *C. reinhardtii* cells at different concentrations for up to 2 h incubations at room temperature and a pH of 5.5 (DI water) using an FDA assay.

Fig. 3A shows the algal cell viability after incubation with various concentrations of CUR-loaded shellac NPs for up to 2 h. Fig. 3A shows that CUR-NPs coated with ODTAB have an extremely high antialgal effect on *C. reinhardtii* even after only 15 min of incubation with algal cell viability decreasing from 94% (control) to 34%, 5%, and 1.5% at 0.0003, 0.0005, and 0.001 wt% CUR-NPs coated with 0.0005, 0.0008 and 0.0017 wt% ODTAB respectively. Note that the non-loaded shellac NPs (no CUR) coated with ODTAB are not toxic to the alae cells at these concentrations (see Fig. S8, ESI†). After 2 h of incubation, all the algal cells died at 0.0005 wt% of CUR-NPs coated with 0.0008 wt% ODTAB and higher concentrations. The anti-yeast effect of CUR loaded shellac NPs was examined for a range of incubation times at pH 5.5 as shown in Fig. 3B. As can be seen in Fig. 3B that yeast cell viability upon incubation with different concentrations of CUR loaded shellac NPs coated with ODTAB has sharply decreased. After 15 min exposure time, the yeast cell viability sharply decreased from 98% to 12% and 2.5% at 0.0005 and 0.001 wt% of CUR loaded in shellac NPs and coated with 0.0008 and 0.0017 wt% ODTAB, respectively, while at higher concentrations of CUR, all cells died. After 2 h, the yeast cell viability was reduced sharply from 98% for the control (no treatment) to 6%, 4%, and 2% at 0.0001, 0.0003, 0.0005 wt%

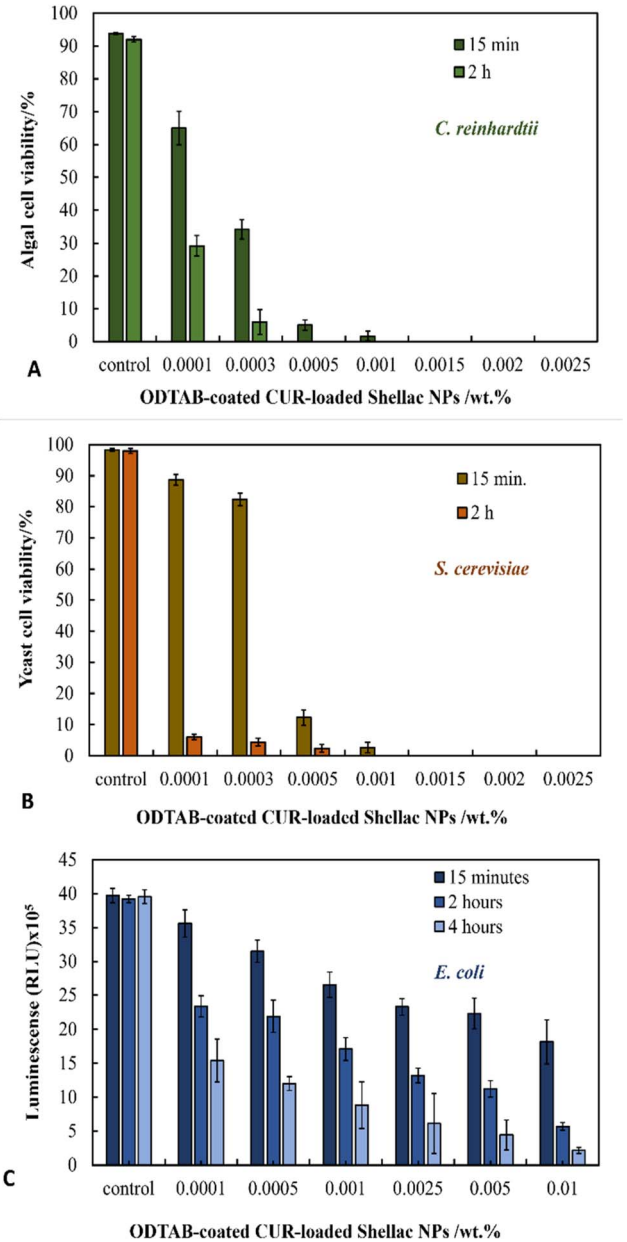

Fig. 3 (A) The viability of algal cells upon incubation at pH 5.5 with different concentrations of CUR loaded shellac NPs coated with ODTAB at room temperature at different incubation time. (B) The cytotoxic effect of different concentrations of CUR loaded shellac NPs coated with ODTAB upon incubation with yeast cells at room temperature at 15 min, and 2 h using FDA assay. (C) The antimicrobial activity of different concentrations of CUR loaded shellac NPs coated with ODTAB against *E. coli* at 15 min, 2 h, and 4 h. These solutions were prepared from a stock solution of 0.03 wt% CUR loaded 0.25 wt% shellac NPs coated with 0.05 wt% ODTAB, ($n = 3$).

CUR loaded in shellac NPs coated with 0.00017, 0.0005, and 0.0008 wt% ODTAB, respectively. CUR has also been reported to have antibacterial activity against many types of bacteria.[46,78,85,86] In this study CUR was encapsulated within shellac NPs, coated with ODTAB and their effect on *E. coli* was evaluated using BacTiter Glo™ luminescence assay. Fig. 3C shows the effect of

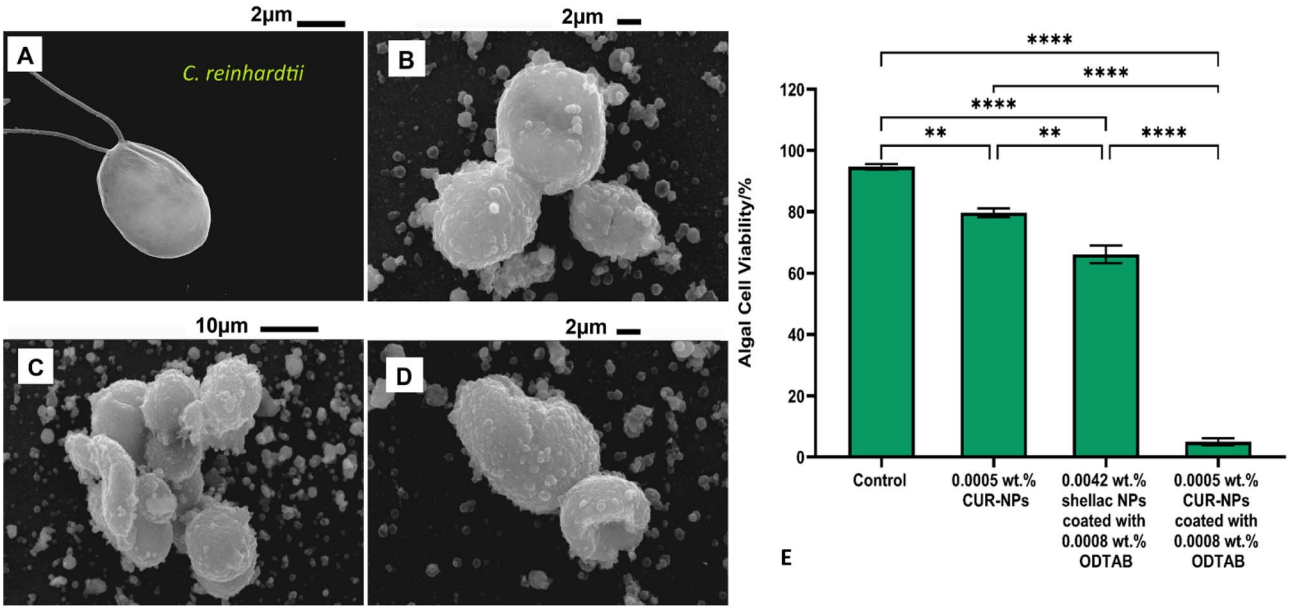

Fig. 4 (A)–(D) SEM images of *C. reinhardtii* where (A) is the control sample (no treatment), (B)–(D) sample incubated cells incubated with 0.0005 wt% CUR loaded shellac NPs coated with 0.0008 wt% ODTAB, after 2 hours incubation at room temperature. (E) *C. reinhardtii* viability upon incubation with: no treatment, 0.0005 wt% non-coated CUR-NPs, 0.0042 wt% shellac NPs (no CUR) coated with 0.0008 wt% ODTAB, 0.0005 wt% CUR-NPs coated with 0.0008 wt% ODTAB, at pH 5.5 and at room temperature for 15 min incubation using the FDA cell viability assay. Data rare given as a mean ± STD from three replicates ($n = 3$). Statistical significance is indicated as follows: ns = not significant; *$p < 0.05$; **$p < 0.01$, ***$p < 0.001$, ****$p < 0.0001$.

encapsulated CUR when incubated with *E. coli* for a period up to 4 h at pH 5.5. The cell viability decreased gradually after 15 minutes incubation, while after 2 hours the antibacterial activity of CUR-NPs coated with ODTAB increased noticeably and the cell viability reduced from 39×10^5 RLU as a control to (6, 4, and 2) x10^5 RLU at 0.0025, 0.005, and 0.01wt% CUR-NPs coated with 0.004, 0.008, and 0.017 wt% ODTAB. After 4 h, the cell viability declined considerably from 40×10^5 RLU for the control to be 2×10^5 RLU at 0.01 wt%, CUR-NPs coated with 0.017 wt% ODTAB. Estimates of MBC can be done from Fig. 3A–C. For example, the MBC for *C. reinhardtii* is in the range 0.001–0.0015% CUR after 15 min, while it drops in the range 0.0003–0.0005% CUR after 2 h, where CUR is formulated in ODTAB-coated CUR-loaded shellac NPs. For *S. cerevisiae* the MBC is between 0.001-0.0015% CUR after 15 min exposure while it drops in the range 0.0005–0.001% CUR after 2 h of incubation. For *E. coli* the MBC is just over 0.01% CUR after 4 h of incubation. Fig. 4A–D shows the SEM images of the *C. reinhardtii* cells after incubation with (0.005 and 0.001) wt% CUR loaded shellac NPs coated with (0.0017 and 0.008) wt% ODTAB after 2 h of incubation. These images show how the NPs encapsulated CUR coated with ODTAB accumulate around the cell due to the positive surface charge of the NPs surface. Fig. 4E compares the antialgal activities of the 0.0005 wt% CUR-NPs, 0.0042 wt% shellac NPs coated with 0.0008 wt% ODTAB, and 0.0005 wt% CUR-NPs coated with 0.0008 wt% ODTAB. This clearly shows that coating the CUR NPs with the ODTAB is more effective. The antimicrobial activity of CUR coated with ODTAB increased due to the positive charge of the complex; this proves the fact that CUR as a surface functionalized nano-formulation acts as a better antialgal agent than the non-coated CUR NPs.

The antifungal activity of CUR loaded shellac NPs coated with ODTAB was examined on yeast at different incubation times at pH 5.5. The *P*-values for all pair of data with respect to control (no treatment) and with respect to the ODTAB-coated CUR NPs are presented the data in Table S1, (ESI†). In the case of ODTAB-coated CUR NPs, the data differences with control, non-coated CUR NPs and non-loaded shellac NPs are all strongly significant. Fig. 5A–D shows the SEM images of the yeast cells incubated with 0.005 wt% of CUR loaded shellac NPs coated with 0.008 wt% for 1 h, the NPs are attracted to the cells and accumulate on their cell walls due to their positive surface charge. In Fig. 5E we compared the anti-yeast activities of non-coated 0.0005 wt% CUR-NPs, 0.0042 wt% shellac NPs coated with 0.0008 wt% ODTAB, and 0.0005 wt% CUR-NPs coated with 0.0008 wt% ODTAB. As observed previously, the anti-yeast activity of CUR-NPs increased after their coating with ODTAB. The *P*-values for all pair of data with respect to control (no treatment) and with respect to the ODTAB-coated CUR NPs are presented the data in Table S2, (ESI†). In the case of ODTAB-coated CUR NPs, the data differences with control, non-coated CUR NPs and non-loaded shellac NPs are all strongly significant.

The surface morphology of *E. coli* cells incubated with 0.001 and 0.005 wt% CUR-NPs coated with 0.0017 and 0.008 wt% ODTAB was examined using scanning electron microscopy as shown in Fig. 6A–D. One can see that the CUR loaded shellac NPs coated with ODTAB were strongly attracted to the cell bacterial cell walls. However, this did not affect the bacteria stronger than the non-coated CUR NPs, most likely due to the

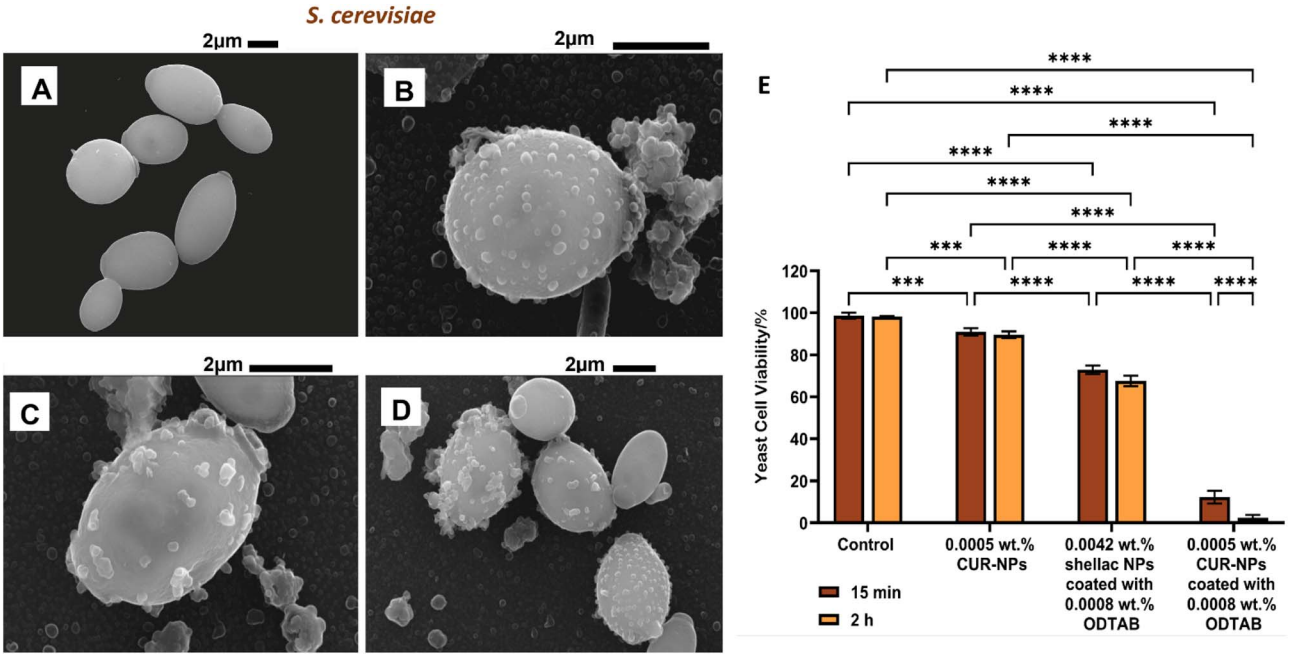

Fig. 5 (A)–(D) SEM images of *S. cerevisiae* with (A) being the control (no treatment), (B)–(D) *S. cerevisiae* incubated yeast cells incubated with 0.0005 wt% CUR loaded shellac NPs coated with 0.0008 wt% ODTAB after 1 h of incubation at room temperature. (E) *S. cerevisiae* cell viability upon incubation with no treatment, 0.0005 wt% non-coated CUR-NPs, 0.0042 wt% shellac NPs (no CUR) coated with 0.0008 wt% ODTAB and 0.0005 wt% CUR-NPs coated with 0.0008 wt% ODTAB at pH 5.5 and at room temperature using FDA assay. Data rare given as a mean ± STD from three replicates ($n = 3$). Statistical significance is indicated as follows: ns = not significant; *$p < 0.05$; **$p < 0.01$, ***$p < 0.001$, ****$p < 0.0001$.

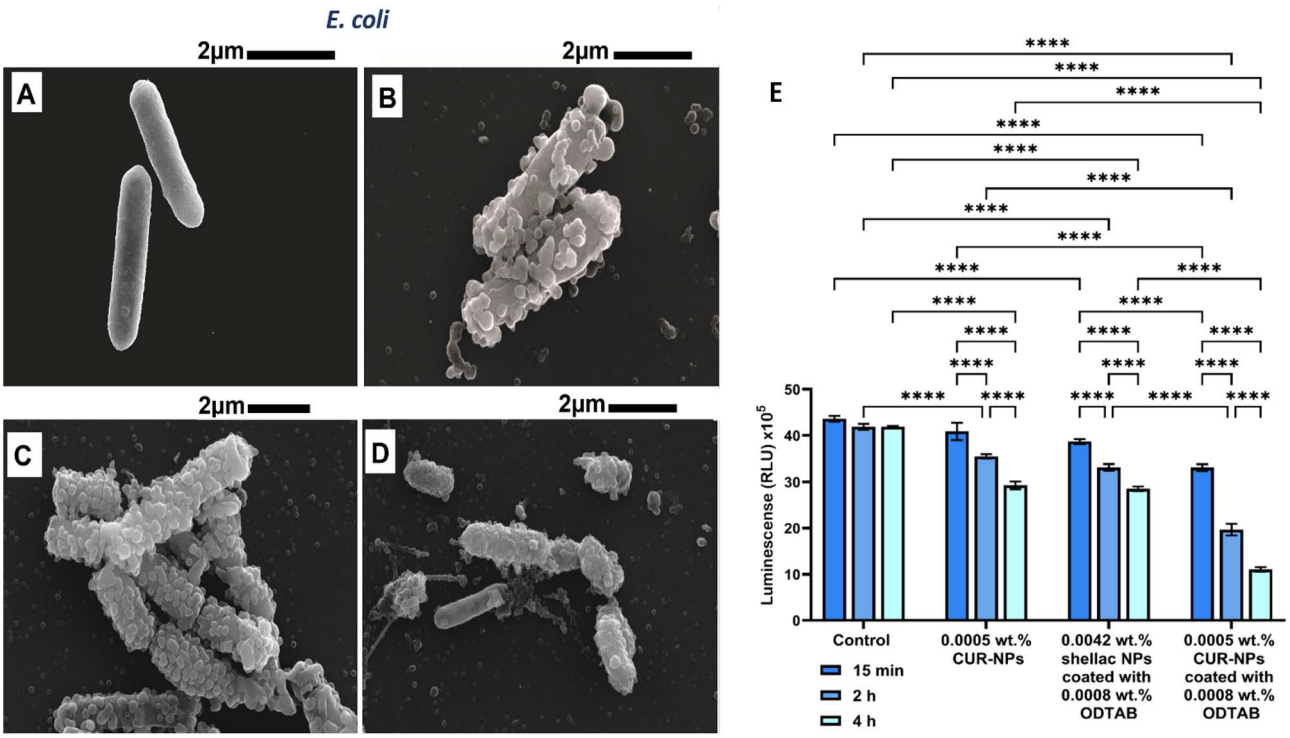

Fig. 6 (A)–(D) SEM images of *E. coli* cells with (A) being the control (no treatment), (B)–(D) *E. coli* incubated with 0.005 wt% CUR-loaded in shellac NPs coated with 0.0008 wt% ODTAB after 2 hours incubation time. (E) The antimicrobial activity of: no-treatment, non-coated 0.0005 wt% CUR-loaded shellac NPs (*), 0.0042 wt% shellac NPs (no CUR) coated with 0.0008 wt% ODTAB (*) and 0.0005 wt% CUR-NPs coated with 0.0008wt% ODTAB (**) towards *E. coli* cells. The incubation was done with a fixed amount of *E. coli* cells at pH 5.5 at room temperature using Bactiter luciferase assay (BacTiter™ Glo, Promega) reagent whose luminescence intensity is directly proportional to the concentration of viable bacteria. Data rare given as a mean ± STD from three replicates ($n = 3$). Statistical significance is indicated as follows: ns = not significant; *$p < 0.05$; **$p < 0.01$, ***$p < 0.001$, ****$p < 0.0001$.

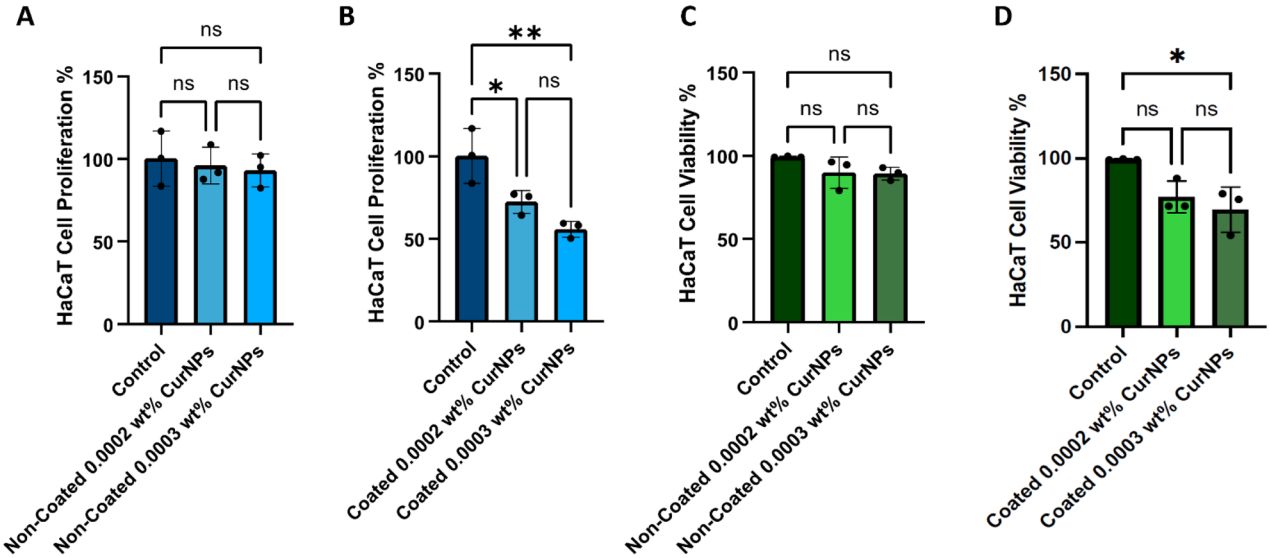

Fig. 7 HaCaT cell proliferation relative to control for (A) non-coated CUR NPs and (B) ODTAB-coated CUR NPs for various CUR concentrations obtained by dilution of the stock 0.05 wt% CUR NPs stock (non-coated and 0.08% ODTAB-coated) with complete DMEM assessed with the MTS assay. HaCAT cell viability relative to control after 24 h incubation with (C) non-coated CUR NPs and (D) ODTAB-coated CUR NPs for various CUR concentrations in complete DMEM obtained by using Hoechst/PI live/dead assay.

slow release of CUR which takes higher NPs concentration to reach the bactericidal concentration of CUR on *E. coli* without accumulation on the bacteria surface due to their negative surface charge. Fig. 6E shows a comparison among all components that were used to formulate the CUR-NPs coated with ODTAB. The *P*-values for all pair of data with respect to control (no treatment) and with respect to the ODTAB-coated CUR NPs and presented the data in Table S3, (ESI†). One can see that in the case of ODTAB-coated CUR NPs, the data differences with control, non-coated CUR NPs and non-loaded shellac NPs are all strongly significant.

Cytotoxicity of ODTAB-coated CUR NPs on human cells

We did additional experiments with human keratinocytes (HaCaT cell line) which were incubated in complete culture for up to 24 h with three different dilutions of ODTAB-coated CUR NPs stock and assessed for the cell proliferation with MTS assay and for cell viability with Hoechst/PI assay. The results are presented in Fig. 7A and B (proliferation) and 7C,D (viability). One can see that although at their highest concentration the ODTAB-coated CUR NPs moderately affect the HaCaT cell proliferation over the course of 24 h incubation, the cell viability remains significantly less affected. Note that there is no effect on both cell proliferation (Fig. 7B) and viability (Fig. 7C) for incubation with the non-coated CUR-NPs.

Conclusions

We have designed a very efficient curcumin nanocarrier based on shellac, a natural and biodegradable material. The role of the nanocarrier design on the antimicrobial activity of the CUR payload was studied after cationic surface functionalisation. Upon ODTAB surface functionalisation of the CUR-loaded shellac NPs, their surface charge changed from negative to positive while maintaining their colloid stability due to the steric interactions of the poloxamer 407 layers. The antimicrobial activity of CUR-loaded shellac nanocarriers was studied upon incubation with microalgae, yeast, and *E. coli* for various time intervals in suspension culture. Optimum conditions were found where the nanocarriers become cationic and still maintained their stability. The antimicrobial activity of these ODTAB-coated shellac NPs loaded with antimicrobial agents showed significantly higher antimicrobial effect than the equivalent overall concentration CUR in non-coated shellac NPs. This effect was attributed to the strong electrostatic adhesion of the ODTAB-coated CUR-loaded NPs with the cell membrane which allowed the antimicrobial agents to be released directly into the microbial cell. Hence, the cationically surface-functionalized nanocarrier provides a boost of the antimicrobial action of the loaded agent. This was amplified by the hydrophobic attraction between the CUR and the shellac matrix of the nanocarriers which slowly releases the CUR. This enhancement effect was due to the strong electrostatic adhesion with the cell membrane which allowed the CUR to be released directly into the microbial cell walls. This type of cationic surface-functionalised shellac nanocarriers could potentially be used as topical antimicrobial therapies to fight antimicrobial resistance, antifungal formulations and advanced biodegradable antialgal solutions.

Data availability

All data regarding this manuscript are already presented in the graphs of the main paper and the ESI† file.

Author contributions

The manuscript was written through contributions of all authors. V. N. P. gave the idea of the study, supervised S. S. A. O. and S. K. and directed the research project, provided the

methodology and created the first draft of the manuscript. S. S. A. O. performed most of the experiments, prepared the figures and the prepared sections of the manuscript. G. M. G. co-supervised the student S. S. A. O., provided technical guidance and methodology, and edited the manuscript. S. K. conducted the experiments on cytotoxicity using human cells and prepared the relevant graphs and protocols. All authors have given approval to the final version of the manuscript.

Conflicts of interest

There are no conflicts of interest to declare.

Acknowledgements

The preparation of this manuscript was supported by Nazarbayev University Faculty Development Competitive Research Grant (No. 040225FD4704, V. N. P.). S. S. M. A. thanks the Iraqi Government, the Higher Committee for Education Development of Iraq and the University of Babylon, Iraq, for the financial support for her PhD study. We are also grateful to Dr Agata Burska at Nazarbayev University for helping with the statistical analysis of the data.

Notes and references

1 A. Goel, A. B. Kunnumakkara and B. B. Aggarwal, *Biochem. Pharmacol.*, 2008, **75**, 787–809.
2 B. B. Aggarwal and B. Sung, *Trends Pharmacol. Sci.*, 2009, **30**, 85–94.
3 S. Zorofchian Moghadamtousi, H. Abdul Kadir, P. Hassandarvish, H. Tajik, S. Abubakar and K. Zandi, *BioMed Res. Int.*, 2014, **2014**, 12.
4 O. P. Sharma, *Biochem. Pharmacol.*, 1976, **25**, 1811–1812.
5 A. J. Ruby, G. Kuttan, K. Dinesh Babu, K. N. Rajasekharan and R. Kuttan, *Cancer Lett.*, 1995, **94**, 79–83.
6 Y. Sugiyama, S. Kawakishi and T. Osawa, *Biochem. Pharmacol.*, 1996, **52**, 519–525.
7 R. C. Srimal and B. N. Dhawan, *J. Pharm. Pharmacol.*, 1973, **25**, 447–452.
8 W. C. Jordan and C. R. Drew, *J. Natl. Med. Assoc.*, 1996, **88**, 333.
9 G. B. Mahady, S. L. Pendland, G. Yun and Z. Z. Lu, *Anticancer Res.*, 2002, **22**, 4179–4181.
10 M. K. Kim, G. J. Choi and H. S. Lee, *J. Agric. Food Chem.*, 2003, **51**, 1578–1581.
11 R. C. Reddy, P. G. Vatsala, V. G. Keshamouni, G. Padmanaban and P. N. Rangarajan, *Biochem. Biophys. Res. Commun.*, 2005, **326**, 472–474.
12 R. Kuttan, P. Bhanumathy, K. Nirmala and M. C. George, *Cancer Lett.*, 1985, **29**, 197–202.
13 B. B. Aggarwal, A. Kumar and A. C. Bharti, *Anticancer Res.*, 2003, **23**, 363–398.
14 S. M. Khopde, K. I. Priyadarsini, P. Venkatesan and M. N. A. Rao, *Biophys. Chem.*, 1999, **80**, 85–91.
15 B. Aggarwal, A. Kumar, M. S. Aggarwal and S. Shishodia, Curcumin Derived from Turmeric (Curcuma longa): a Spice for All Seasons, in *Phytopharmaceuticals in Cancer Chemoprevention*, 2004, pp. 349–388.
16 F. Yang, G. P. Lim, A. N. Begum, O. J. Ubeda, M. R. Simmons, S. S. Ambegaokar, P. P. Chen, R. Kayed, C. G. Glabe, S. A. Frautschy and G. M. Cole, *J. Biol. Chem.*, 2005, **280**, 5892–5901.
17 A. Ukil, S. Maity, S. Karmakar, N. Datta, J. R. Vedasiromoni and P. K. Das, *Br. J. Pharmacol.*, 2003, **139**, 209–218.
18 M. E. Egan, M. Pearson, S. A. Weiner, V. Rajendran, D. Rubin, J. Glockner-Pagel, S. Canny, K. Du, G. L. Lukacs and M. J. Caplan, *Science*, 2004, **304**, 600–602.
19 M. C. Heng, M. K. Song, J. Harker and M. K. Heng, *Br. J. Dermatol.*, 2000, **143**, 937–949.
20 E. Tourkina, P. Gooz, J. C. Oates, A. Ludwicka-Bradley, R. M. Silver and S. Hoffman, *Am. J. Respir. Cell Mol. Biol.*, 2004, **31**, 28–35.
21 O. Naksuriya, S. Okonogi, R. M. Schiffelers and W. E. Hennink, *Biomaterials*, 2014, **35**, 3365–3383.
22 R. Löbenberg and J. Kreuter, *AIDS Res. Hum. Retroviruses*, 1996, **12**, 1709–1715.
23 P. H. Hoet, I. Brüske-Hohlfeld and O. V. Salata, *J. Nanobiotechnol.*, 2004, **2**, 1–15.
24 A. Kunwar, A. Barik, R. Pandey and K. I. Priyadarsini, *Biochim. Biophys. Acta*, 2006, **1760**, 1513–1520.
25 S. Bisht, G. Feldmann, S. Soni, R. Ravi, C. Karikar, A. Maitra and A. Maitra, *J. Nanobiotechnol.*, 2007, **5**, 3.
26 K. Sou, S. Inenaga, S. Takeoka and E. Tsuchida, *Int. J. Pharm.*, 2008, **352**, 287–293.
27 V. Kumar, S. A. Lewis, S. Mutalik, D. B. Shenoy and V. N. Udupa, *Indian J. Physiol. Pharmacol.*, 2002, **46**, 209–217.
28 S. Salmaso, S. Bersani, A. Semenzato and P. Caliceti, *J. Drug Targeting*, 2007, **15**, 379–390.
29 P. K. Vemula, J. Li and G. John, *J. Am. Chem. Soc.*, 2006, **128**, 8932–8938.
30 Z. Ma, A. Shayeganpour, D. R. Brocks, A. Lavasanifar and J. Samuel, *Biomed. Chromatogr.*, 2007, **21**, 546–552.
31 A. Sahu, U. Bora, N. Kasoju and P. Goswami, *Acta Biomater.*, 2008, **4**, 1752–1761.
32 R. K. Das, N. Kasoju and U. Bora, *Nanomed. Nanotechnol. Biol. Med.*, 2010, **6**, 153–160.
33 A. Karewicz, D. Bielska, A. Loboda, B. Gzyl-Malcher, J. Bednar, A. Jozkowicz, J. Dulak and M. Nowakowska, *Colloids Surf., B*, 2013, **109**, 307–316.
34 M. Sun, X. Su, B. Ding, X. He, X. Liu, A. Yu, H. Lou and G. Zhai, *Nanomedicine*, 2012, **7**, 1085–1100.
35 F. Danhier, E. Ansorena, J. M. Silva, R. Coco, A. Le Breton and V. Préat, *J. Controlled Release*, 2012, **161**, 505–522.
36 S. Fredenberg, M. Wahlgren, M. Reslow and A. Axelsson, *Int. J. Pharm.*, 2011, **415**, 34–52.
37 R. A. Jain, *Biomaterials*, 2000, **21**, 2475–2490.
38 J. M. Anderson and M. S. Shive, *Adv. Drug Delivery Rev.*, 1997, **28**, 5–24.
39 J. Shaikh, D. D. Ankola, V. Beniwal, D. Singh and M. N. V. R. Kumar, *Eur. J. Pharm. Sci.*, 2009, **37**, 223–230.
40 L. Song, Y. Shen, J. Hou, L. Lei, S. Guo and C. Qian, *Colloids Surf., A*, 2011, **390**, 25–32.

41 H. Tang, C. J. Murphy, B. Zhang, Y. Shen, M. Sui, E. A. Van Kirk, X. Feng and W. J. Murdoch, *Nanomedicine*, 2010, **5**, 855–865.
42 L. Mayol, C. Serri, C. Menale, S. Crispi, M. T. Piccolo, L. Mita, S. Giarra, M. Forte, A. Saija, M. Biondi and D. G. Mita, *Eur. J. Pharm. Biopharm.*, 2015, **93**, 37–45.
43 X. Yang, Z. Li, N. Wang, L. Li, L. Song, T. He, L. Sun, Z. Wang, Q. Wu, N. Luo, C. Yi and C. Gong, *Sci. Rep.*, 2015, **5**, 10322.
44 W. Tiyaboonchai, W. Tungpradit and P. Plianbangchang, *Int. J. Pharm.*, 2007, **337**, 299–306.
45 Y. Yuan, S. Zhang, M. Ma, Y. Xu and D. Wang, *Food Chem.:X*, 2022, **15**, 100431.
46 D. Zhuang, Y. Wang, S. Wang, R. Li, H. N. Ahmad and J. Zhu, *Int. J. Biol. Macromol.*, 2024, **268**, 131607.
47 R. Prasad and S. C. Sengupta, *J. Oil Colour Chem. Assoc.*, 1978, **61**, 49–51.
48 S. Limmatvapirat, C. Limmatvapirat, M. Luangtana-anan, J. Nunthanid, T. Oguchi, Y. Tozuka, K. Yamamoto and S. Puttipipatkhachorn, *Int. J. Pharm.*, 2004, **278**, 41–49.
49 I. J. Ogaji, E. I. Nep and J. D. Audu-Peter, *Pharm. Anal. Acta*, 2012, **3**, 146.
50 R. C. Rowe, P. J. Sheskey and P. J. Weller, *Handbook of Pharmaceutical Excipients*, Pharmaceutical Press; American Pharmaceutical Association, London; Chicago: Washington, DC, England, 4th edn, 2003.
51 H. S. Cockeram and S. A. Levine, *J. Soc. Cosmet. Chem.*, 1961, **12**, 316–323.
52 K. Krause and R. Müller, *Int. J. Pharm.*, 2001, **223**, 89–92.
53 A. Patel, P. Heussen, J. Hazekamp and K. P. Velikov, *Soft Matter*, 2011, **7**, 8549.
54 P. Kraisit, S. Limmatvapirat, J. Nunthanid, P. Sriamornsak and M. Luangtana-anan, *Pharm. Dev. Technol.*, 2013, **18**, 686–693.
55 S. S. M. Al-Obaidy, G. M. Greenway and V. N. Paunov, *Nanoscale Adv.*, 2019, **1**, 858–872.
56 S. S. M. Al-Obaidy, G. M. Greenway and V. N. Paunov, *J. Mater. Chem. B*, 2019, **7**, 3119–3133.
57 S. S. M. Al-Obaidy, G. M. Greenway and V. N. Paunov, *Pharmaceutics*, 2021, **13**, 1389.
58 P. J. Weldrick, M. J. Hardman and V. N. Paunov, *Adv. NanoBiomed Res.*, 2021, **1**, 2000027.
59 P. J. Weldrick, M. J. Hardman and V. N. Paunov, *ACS Appl. Mater. Interfaces*, 2019, **11**, 43902–43919.
60 P. J. Weldrick, M. J. Hardman and V. N. Paunov, *Mater. Chem. Front.*, 2021, **5**, 961–972.
61 P. J. Weldrick, S. San and V. N. Paunov, *ACS Appl. Nano Mater.*, 2021, **4**, 1187–1201.
62 P. J. Weldrick, S. Iveson, M. J. Hardman and V. N. Paunov, *Nanoscale*, 2019, **11**, 10472–10485.
63 M. J. Al-Awady, P. J. Weldrick, M. J. Hardman, G. M. Greenway and V. N. Paunov, *Mater. Chem. Front.*, 2018, **2**, 2032–2044.
64 P. J. Weldrick, A. Wang, A. F. Halbus and V. N. Paunov, *Nanoscale*, 2022, **14**, 4018–4041.
65 E. O. Asare, E. A. Mun, E. Marsili and V. N. Paunov, *J. Mater. Chem. B*, 2022, **10**, 5129–5153.
66 A. Wang, P. J. Weldrick, L. A. Madden and V. N. Paunov, *ACS Appl. Nano Mater.*, 2021, **13**, 22182–22194.
67 A. Wang, P. J. Weldrick, L. A. Madden and V. N. Paunov, *Biomater. Sci.*, 2021, **9**, 6927.
68 S. K. Sharma, S. K. Shukla and D. N. Vaid, *Def. Sci. J.*, 1983, **33**, 261–271.
69 W. H. Gardner and W. F. Whitmore, *Ind. Eng. Chem.*, 1929, **21**, 226–229.
70 P. Alexandridis and T. Alan Hatton, *Colloids Surf., A*, 1995, **96**, 1–46.
71 P. Tyagi, M. Singh, H. Kumari, A. Kumari and K. Mukhopadhyay, *PLoS One*, 2015, **10**, e0121313.
72 S. H. Mun, D. K. Joung, Y. S. Kim, O. H. Kang, S. B. Kim, Y. S. Seo, Y. C. Kim, D. S. Lee, D. W. Shin, K. T. Kweon and D. Y. Kwon, *Phytomedicine*, 2013, **20**, 714–718.
73 M. Sharma, R. Manoharlal, N. Puri and R. Prasad, *Antimicrob. Agents Chemother.*, 2010, **54**, 4732–4742.
74 P. Kraisit, S. Limmatvapirat, J. Nunthanid, P. Sriamornsak and M. Luangtana-anan, *Pharm. Dev. Technol.*, 2013, **18**, 686–693.
75 A. A. K. Das, M. M. N. Esfahani, O. D. Velev, N. Pamme and V. N. Paunov, *J. Mater. Chem. A*, 2015, **3**, 20698–20707.
76 A. F. Halbus, T. S. Horozov and V. N. Paunov, *ACS Appl. Nano Mater.*, 2020, **3**, 440–451.
77 M. J. Al-Awady, A. Fauchet, G. M. Greenway and V. N. Paunov, *J. Mater. Chem. B*, 2017, **5**, 7885–7897.
78 P. Anand, A. B. Kunnumakkara, R. A. Newman and B. B. Aggarwal, *Mol. Pharm.*, 2007, **4**, 807–818.
79 R. K. Basniwal, H. S. Buttar, V. Jain and N. Jain, *J. Agric. Food Chem.*, 2011, **59**, 2056–2061.
80 D. Chen, C.-X. Zhao, C. Lagoin, M. Hai, L. Arriaga, S. Koehler, A. Abbaspourrad and D. A. Weitz, *R. Soc. Open Sci.*, 2017, **4**, 170919.
81 Y.-J. Wang, M.-H. Pan, A.-L. Cheng, L.-I. Lin, Y.-S. Ho, C.-Y. Hsieh and J.-K. Lin, *J. Pharm. Biomed. Anal.*, 1997, **15**, 1867–1876.
82 J. Shubham, M. Sai Rama Krishna and C. Kaushik, *Biomed. Mater.*, 2016, **11**, 055007.
83 P. R. K. Mohan, G. Sreelakshmi, C. V. Muraleedharan and R. Joseph, *Vib. Spectrosc.*, 2012, **62**, 77–84.
84 A. Ahmed, J. Hearn, W. Abdelmagid and H. Zhang, *J. Mater. Chem.*, 2012, **22**, 25027–25035.
85 P. La Colla, E. Tramontano, C. Musiu, M. Marongiu, E. Novellino, G. Greco, S. Massa, R. Di Santo, R. Costi and A. Marino, *Antiviral Res.*, 1998, **37**, 57.
86 L. Ammayappan and J. J. Moses, *Fibers Polym.*, 2009, **10**, 161–166.